Observation of horizontal temperature variations by a limb-sounding spatial heterodyne interferometer

Konstantin F.F. Ntokas[a], Jörn Ungermann[a], Martin Kaufmann[a], Tom Neubert[b], and Martin Riese[a]

[a]Institute of Energy and Climate Research (IEK-7), Research Center Juelich, Juelich, Germany
[b]Central Institute for Engineering, Electronics and Analytics, Electronic Systems (ZEA-2), Research Centre Juelich, Juelich, Germany

ABSTRACT

A limb-viewing spatial heterodyne interferometer is developed to observe temperature in the mesosphere and lower thermosphere. This can be used to measure atmospheric waves with small vertical wavelengths. The instrument measures the O_2 atmospheric A-band airglow emission in the near-infrared. The emission is visible during day- and night-time, allowing for a continuous observation. The image is taken by a 2d detector. The optical system conserves the 2d spatial temperature information. The spectral information is superimposed in horizontal detector direction. The usual processing thus uses the horizontal detector dimension to resolve the spectral while averaging the underlying spatial information. The altitude coverage is given by the vertical detector direction, resulting in a finely resolved vertical temperature profile for one image.

In light of this, we explore a novel processing approach that exploits the spatial information along the horizontal axis as well. We propose to split the interferogram into two halves, mirror it around the center and perform a retrieval on both sides separately, obtaining two spatial cross tracks of independent temperature data. Assuming that the instrument views backward, consecutive measurements give along track sampling. Combining this with the split interferogram method and the usual fine vertical resolution of the instrument, it provides 3d information on the atmospheric temperature field which allows to obtain some information on 3d propagation characteristics of atmospheric waves.

In our research, we delve into the viability, advantages and constraints of the split interferogram approach. We will discuss the impact of horizontal temperature variation onto the retrieval result. We show the impact of background temperatures on the retrieval. Furthermore, we discuss the influence of apodization onto the retrieval of split interferograms.

Keywords: Atmospheric Remote Sensing, Fourier transform spectroscopy, CubeSats, spatial heterodyne interferometer, single-sided interferogram

1. INTRODUCTION

The dynamical structure of the mesosphere and lower thermosphere (MLT) is primarily influenced by atmospheric waves like planetary waves, tides, and gravity waves.[1] Gravity waves transfer energy from lower altitudes to the MLT region. Common sources of gravity waves in the lower atmosphere include uplift of air masses due to orography, convection, and unstable jets, while higher altitude sources remain less understood but can significantly impact the MLT region.[2] Global circulation models typically parameterize small and medium-scale gravity waves.[3]

To measure temperature in the MLT region, O_2 $(0,0)$ atmospheric A-band emissions at 762 nm are utilized.[4–7] A limb sounding spatial heterodyne interferometer (SHI) is developed collaboratively by the Jülich Research Center and the University of Wuppertal in Germany.[8] The instrument derives temperature from relative intensities of the emission lines, eliminating the need for absolute radiometric calibration and easing the calibration process. This emission is observable during the day and partly at night.

Further author information: (Send correspondence to K. Ntokas)
K. Ntokas.: E-mail: k.ntokas@fz-juelich.de, Telephone: +49 2461 611840

Remote Sensing of Clouds and the Atmosphere XXVIII, edited by Adolfo Comerón, Evgueni I. Kassianov, Klaus Schäfer, Richard H. Picard, Konradin Weber, Proc. of SPIE Vol. 12730, 127300K · © The Authors.
Published under a Creative Commons Attribution CC-BY 3.0 License· doi: 10.1117/12.2679980

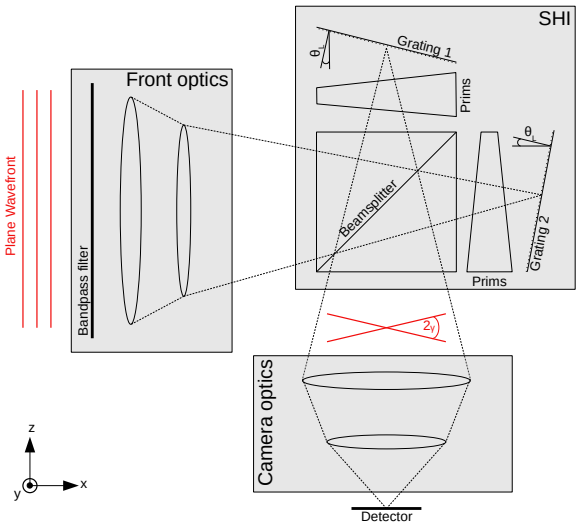

Figure 1: Schematic of the SHS instrument

The instrument functions like a camera, mapping the atmospheric scene onto the detector. The SHI is used to detect the spectrum of the O_2 A-band emissions, superimposing spectral information along the horizontal detector axis. Traditional processing extracts spectral information along the horizontal direction and spatial information along the vertical direction, generating a finely resolved 1-D temperature profile from a single image, which can be used to derive wave parameters.[9,10]

To exploit additional spatial information in the horizontal direction, a new processing method is proposed, enabling the retrieval of two 1-D temperature profiles from one image using single-sided interferograms, mirrored at the center. This method would allow for resolving medium-scale gravity waves.[10] The paper presents the details of this methodology, starting with the introduction of the instrument in Sec.2 followed by an assessment of the novel processing method using single-sided interferograms in Sec. 3. Hereby, we look at the temperature sensitivity of the retrieval with respect to the temperature variation in horizontal direction in Sec. 3.1. Further, we assess the locations of the retrieved temperatures using half interferograms for simulated horizontal temperature variations in Sec. 3.2. At last we assess the effect of apodization onto the retrieval using half interferograms in Sec. 3.3.

2. SPATIAL HETERODYNE INTERFEROMETER

The spatial heterodyne interferometer (SHI) operates similarly to a Michelson interferometer, but instead of using two mirrors, it utilizes fixed tilted gratings.[11–14] Figure 1 presents a schematic of the SHI instrument. Incident light is directed by front optics onto diffraction gratings after passing through a beam splitter. Camera optics then image the gratings onto a 2-dimensional focal plane array (FPA). The tilt angle of the wave fronts, and consequently the interference pattern frequency on the FPA depends on the frequency of the incoming light. Multiple emission lines create superimposed cosine waves across the FPA in the horizontal detector dimension. A single measurement therefore contains spatial information along the vertical and superimposed spectral and spatial information along the horizontal detector axis, corresponding to the vertical and horizontal across-track axis in the atmosphere.

Mathematically, a 1D interferogram can be described by[12,15,16]

$$I(x) = \int_{b0}^{b1} S(\sigma, x)\,[1 + \cos(2\pi f(\sigma)x)]\,d\sigma, \tag{1}$$

where $S(\sigma, x)$ is the radiance variation across the horizontal field of view and and $[b_0, b_1]$ define the spectral limit of the bandpass filter. The spatial frequency f corresponds to the wavenumber by $f(\sigma) = 4(\sigma - \sigma_L)\tan\theta_L M$,

where σ_L and θ_L are the Littrow wavenumber and Littrow angle, respectively, and M is the magnification factor of the camera optics. The specification of the current instrument version is given in Tab. 1.

Table 1: Summary of instrument specification

Parameter	Property
Littrow wavenumber	$13\,047\,\mathrm{cm}^{-1}$
Littrow angle	$6.6°$
Magnification factor of camera optics	0.57
Groove density of gratings	$300\,\mathrm{mm}^{-1}$
Spectral range	$13\,059\,\mathrm{cm}^{-1}$ to $13\,166\,\mathrm{cm}^{-1}$
Field of view	$1.3\,\mathrm{deg}^2$
	($\approx 60\,\mathrm{km}^2$ for orbit altitude of 600 km)
Detector columns/rows	860/860
Pixel pitch	11 µm

3. RETRIEVAL OF HORIZONTAL TEMPERATURE VARIATION

In the conventional processing, a Fourier transformation is applied along the x-axis to convert it into a spectrum, and inverse modeling is used to derive the temperature from the spectral signature. In contrast, our proposed processing method involves splitting the interferogram and mirroring it around the center, taking advantage of its symmetry. This yields two interferograms, enabling the extraction of an averaged temperature for both the left and right sides of the field of view, resulting in two temperature retrieval results per altitude layer. First examples showed the feasibility of this method.[10] However, the difference between the two retrieved temperatures was found to be closer than what the mean temperature of each side suggested. This discrepancy is attributed to larger deviation from the mean intensity around the center of the interferogram, which have a more significant impact on the retrieved temperature.[17]

To further validate and generalize these results, we conducted a sensitivity study in Sec.3.1, focusing on the temperature retrieval's sensitivity to horizontal temperature variations. In Section 3.2, we carry out a retrieval using the split interferogram method on an extensive collection of horizontal temperature fluctuations, commonly produced by gravity waves. Finally, in Sec. 3.3, we investigated the influence of apodization on the retrieval process.

3.1 Sensitivity to horizontal temperature variations

In this section, we evaluate the sensitivity of the temperature retrieval to horizontal temperature variations. Our goal is to estimate how the retrieved temperature changes in response to localized temperature changes along the horizontal across-track axis. The results, presented in Figure 2a, display a wavy pattern reflecting the varying intensities of emission lines and their modulation through the instrument. It is evident from the matrix that the retrieved temperature is most sensitive to temperatures close to the main lobe, regardless of the temperature level. To further analyze this sensitivity, we present smoothed rows of the matrix in Figure 2b. For lower temperatures below 300 K, the sensitivity is lower around the main lobe and higher towards the sides. Temperature levels around 500 K, corresponding to temperatures in the lower thermosphere, exhibit the highest sensitivity at the central peak and the lowest sensitivity towards the sides. This effect diminishes for temperatures above 500 K. Consequently, the temperature retrieval is least sensitive to horizontal temperature variations around 500 K.

3.2 Temperature retrieval of horizontal temperature variations

To get a comprehensive picture, we perform a split field of view retrieval of interferograms incorporating temperature variations typically caused by gravity waves. Hereby, we model a sinusoidal horizontal temperature variation with parameters like background temperature, amplitude, horizontal wavelength, and phase.

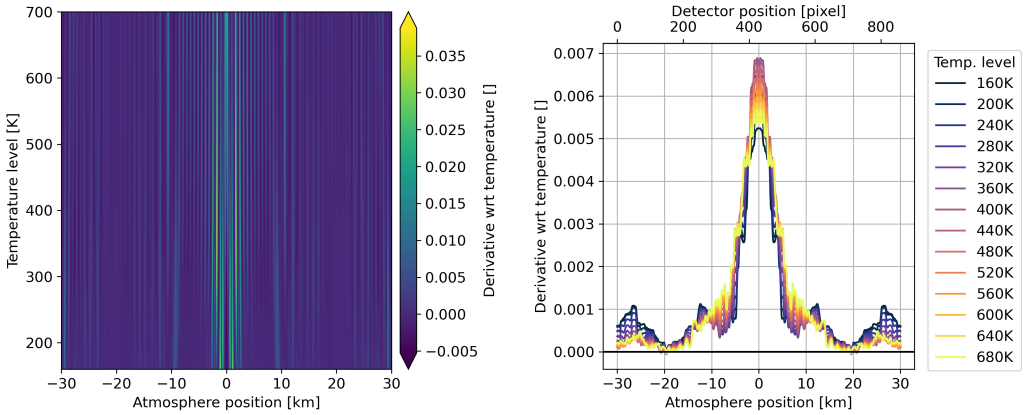

(a) (b)

Figure 2: (a) Derivative of temperature at a given horizontal position for multiple temperature levels; (b) Selected rows of (a) and smoothed by a running mean with window size 101

For the further analysis we introduce the term 'location' of a retrieved temperature, which is defined by the abscissa of that atmospheric model temperature, which is equal to the retrieved one. The distance between the locations of each side serves as a measure of how well the presence of a horizontal temperature variation can be characterized. The results are displayed in Figure 3. The amplitude of the temperature variation, shown in Figure 3a, has no influence on the retrieved temperatures' location. However, the temperature background (Figure 3b) affects the distance of the retrieved temperatures due to varying sensitivities of the O_2 A-band emission with respect to temperatures, as explained in Sec. 3.1. Regarding the phase (Figure 3c), $\phi = 0$ and $\phi = \pi$ represent the crest and trough of the captured temperature residual. In these cases, the temperature variation is low at the center and large at the edges, which works against the increased temperature information around the center and results in temperatures being further apart from each other. The horizontal wavelength of the temperature variation slightly affects the distance of the retrieved temperatures (Figure 3d). Short wavelengths result in a wider distribution of locations because the phase has a more pronounced influence.

In conclusion, accounting for the background temperature and the phase allows for a good estimate of the location of the retrieved temperature and therefore a reliable base for deriving the horizontal wave parameter components.

3.3 Influence of apodization

Apodization is a common practice in Fourier transform spectroscopy, aiming to modify the instrument line shape (ILS) to minimize the spurious side lobes of the sinc-function (Figure 4b, Norton-Beer 1.0, representing the usual ILS without apodization).[18] By doing so, apodization enhances the localization of spectral information as shown in Fig. 4b, making the measurements more robust against instrumental errors. However, apodization comes with the trade-off of reduced spectral resolution, as it decreases the side lobes. In this analysis, the Norton-Beer apodization functions (Figure4)[19–21] are utilized, which are widely popular in Fourier transform spectroscopy.[22,23]

To investigate the impact of apodization on split field of view retrievals, we conducted simulations with a linear horizontal temperature variation at various background temperature levels and apodization strengths. The results are depicted in Figure 5. When using the full interferogram, we were able to recover the mean temperature for each temperature level, independent of the apodization strength. However, for single-sided interferograms, stronger apodization reduced the localization difference between the retrieved temperatures of the left and right side. This effect can be understood by revisiting Figure 4a, where apodization decreases the interferogram's intensity towards the edges, placing a greater weight on the central information content. As explained in Sec. 3.1, this amplifies the tendency of retrieved temperatures to be closer to the center. The case

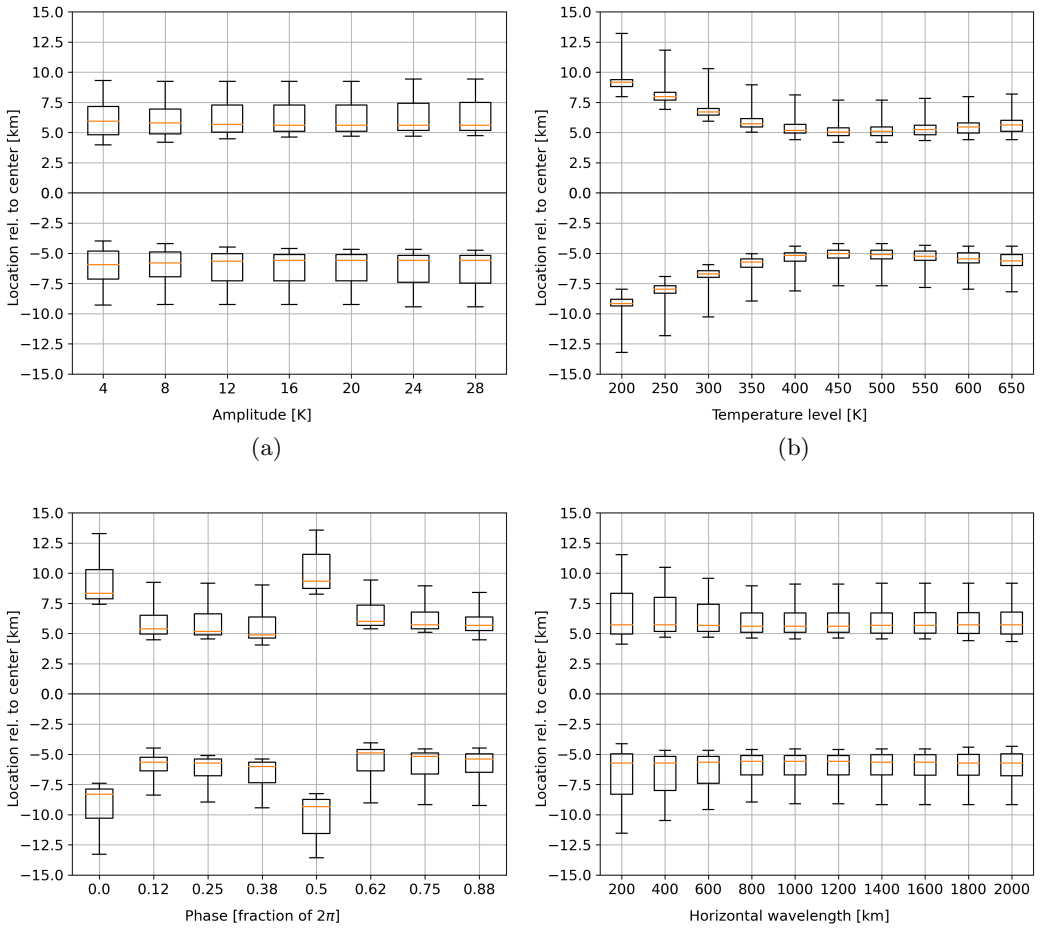

Figure 3: Relative location of the retrieved temperatures within the temperature variation using single sided interferograms (a) for varying amplitude, (b) for varying temperature background level, (c) for varying horizontal wavelength and (d) for varying phase; the box extends from the lower to upper quartile values, the whiskers extend from the 5th to 95th percentile;

without apodization (Norton-Beer 1.0) exhibited a decrease in the temperature difference between the two sides for temperature levels between 160 K and 500 K, followed by a slight increase for higher temperatures. This observation aligns with the results shown in Figure 3b.

In conclusion, when using mirrored single-sided interferograms, apodization becomes not only a trade-off between spectral resolution and spectral confinement but also between spatial resolution of the two retrieved horizontal temperature data points and robustness against errors. Hence, using single-sided interferograms imposes higher requirements for instrument error mitigation if one aims to maintain a significant across-track distance between the two retrieved temperature data points.

4. CONCLUSION

This study explores the potential of a novel processing method that enables the retrieval of horizontal across-track temperature variations using the presented SHI limb-sounder. With this approach, two temperature profiles distributed across-crack can be obtained instead of the usual single profile. Upon examining the impact of horizontal temperature variations across the field of view, we found that the retrieved temperatures tend to be closer to the center of the field of view. A sensitivity study of the retrieved temperature for a given temperature

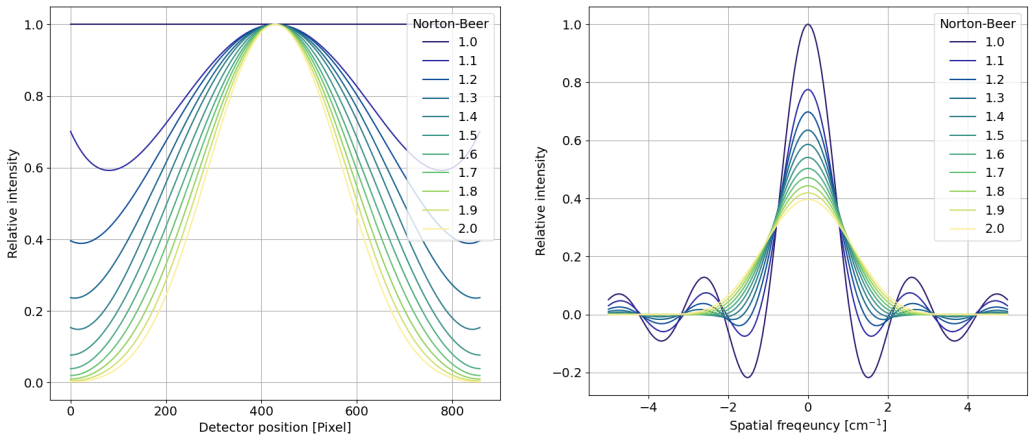

(a) (b)

Figure 4: Apodization functions used for the assessment;[19] (a) apodization function in the spatial domain; (b) apodization function in the spectral domain;

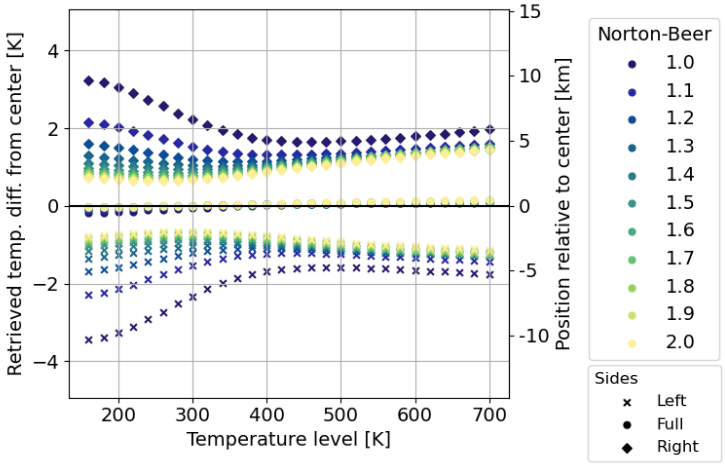

Figure 5: Retrieved temperatures using a linear temperature gradient for multiple temperature levels and different strengths of apodization; the number refers to the full width half maximum (FWHM) of the apodization function relative to the sinc function and thus higher number means stronger apodization;

variation revealed that the majority of temperature information is concentrated around the interferogram's center. Additionally, we found that apodization impacts the spatial resolution of the data obtained through this method. Generally, weaker apodization provides better spatial resolution across the line of sight, although it needs to be carefully balanced against model or instrumental uncertainties. In practical terms, this method allows for the horizontal resolution of medium-scale gravity waves from such data.[10] However, it is essential to consider that the phase and background temperature of the captured wave can affect the location of the retrieved temperatures.

ACKNOWLEDGMENTS

This project 19ENV07 MetEOC-4 has received funding from the EMPIR programme co-financed by the Participating States and from the European Union's Horizon 2020 research and innovation programme.

REFERENCES

[1] Vincent, R. A., "The dynamics of the mesosphere and lower thermosphere: a brief review," *Progress in Earth and Planetary Science* **2**, 4 (Mar. 2015).

[2] Becker, E. and Vadas, S. L., "Explicit Global Simulation of Gravity Waves in the Thermosphere," *Journal of Geophysical Research: Space Physics* **125** (Oct. 2020).

[3] Alexander, M. J., Geller, M., McLandress, C., Polavarapu, S., Preusse, P., Sassi, F., Sato, K., Eckermann, S., Ern, M., Hertzog, A., Kawatani, Y., Pulido, M., Shaw, T. A., Sigmond, M., Vincent, R., and Watanabe, S., "Recent developments in gravity-wave effects in climate models and the global distribution of gravity-wave momentum flux from observations and models: Recent Developments in Gravity-Wave Effects," *Quarterly Journal of the Royal Meteorological Society* **136**, 1103–1124 (July 2010).

[4] Ortland, D. A., Hays, P. B., Skinner, W. R., and Yee, J.-H., "Remote sensing of mesospheric temperature and $O_2(^1\Sigma)$ band volume emission rates with the high-resolution Doppler imager," *Journal of Geophysical Research: Atmospheres* **103**, 1821–1835 (Jan. 1998).

[5] Sheese, P., [*Mesospheric ozone densities retrieved from OSIRIS observations of the oxygen A-band dayglow*] (2009). ISBN: 9780494649367.

[6] Englert, C. R., Harlander, J. M., Brown, C. M., Marr, K. D., Miller, I. J., Stump, J. E., Hancock, J., Peterson, J. Q., Kumler, J., Morrow, W. H., Mooney, T. A., Ellis, S., Mende, S. B., Harris, S. E., Stevens, M. H., Makela, J. J., Harding, B. J., and Immel, T. J., "Michelson Interferometer for Global High-Resolution Thermospheric Imaging (MIGHTI): Instrument Design and Calibration," *Space Science Reviews* **212**, 553–584 (Oct. 2017).

[7] Gumbel, J., Megner, L., Christensen, O. M., Ivchenko, N., Murtagh, D. P., Chang, S., Dillner, J., Ekebrand, T., Giono, G., Hammar, A., Hedin, J., Karlsson, B., Krus, M., Li, A., McCallion, S., Olentšenko, G., Pak, S., Park, W., Rouse, J., Stegman, J., and Witt, G., "The MATS satellite mission – gravity wave studies by Mesospheric Airglow/Aerosol Tomography and Spectroscopy," *Atmospheric Chemistry and Physics* **20**, 431–455 (Jan. 2020).

[8] Kaufmann, M., Olschewski, F., Mantel, K., Solheim, B., Shepherd, G., Deiml, M., Liu, J., Song, R., Chen, Q., Wroblowski, O., Wei, D., Zhu, Y., Wagner, F., Loosen, F., Froehlich, D., Neubert, T., Rongen, H., Knieling, P., Toumpas, P., Shan, J., Tang, G., Koppmann, R., and Riese, M., "A highly miniaturized satellite payload based on a spatial heterodyne spectrometer for atmospheric temperature measurements in the mesosphere and lower thermosphere," *Atmospheric Measurement Techniques* **11**, 3861–3870 (July 2018).

[9] Ern, M., "Absolute values of gravity wave momentum flux derived from satellite data," *Journal of Geophysical Research* **109**(D20), D20103 (2004).

[10] Chen, Q., Ntokas, K., Linder, B., Krasauskas, L., Ern, M., Preusse, P., Ungermann, J., Becker, E., Kaufmann, M., and Riese, M., "Satellite observations of gravity wave momentum flux in the mesosphere and lower thermosphere (MLT): feasibility and requirements," *Atmospheric Measurement Techniques* **15**, 7071–7103 (Dec. 2022).

[11] Connes, P., "Spectromètre interférentiel à sélection par l'amplitude de modulation," *Journal de Physique et le Radium* **19**(3), 215–222 (1958).

[12] Harlander, J., Reynolds, R. J., and Roesler, F. L., "Spatial heterodyne spectroscopy for the exploration of diffuse interstellar emission lines at far-ultraviolet wavelengths," *The Astrophysical Journal* **396**, 730 (Sept. 1992).

[13] Cardon, J., Englert, C., Harlander, J., Roesler, F., and Stevens, M., "SHIMMER on STS-112: Development and Proof-of-Concept Flight," in [*AIAA Space 2003 Conference & Exposition*], American Institute of Aeronautics and Astronautics, Long Beach, California (Sept. 2003).

[14] Watchorn, S., Roesler, F. L., Harlander, J. M., Jaehnig, K. P., Reynolds, R. J., and Sanders III, W. T., "Development of the spatial heterodyne spectrometer for VUV remote sensing of the interstellar medium," in [*UV/EUV and Visible Space Instrumentation for Astronomy and Solar Physics,*], Siegmund, O. H. W., Fineschi, S., and Gummin, M. A., eds., 284–295, Proc. SPIE 4498, San Diego, CA (Dec. 2001).

[15] Smith, B. W. and Harlander, J. M., "Imaging spatial heterodyne spectroscopy: theory and practice," in [*Infrared Technology and Applications XXV*], Andresen, B. F. and Strojnik, M., eds., 925, Proc. SPIE 3698, Orlando, FL (July 1999).

[16] Cooke, B. J., Smith, B. W., Laubscher, B. E., Villeneuve, P. V., and Briles, S. D., "Analysis and system design framework for infrared spatial heterodyne spectrometers," in [*Infrared Imaging Systems: Design, Analysis, Modeling, and Testing X*], Holst, G. C., ed., 167–191, Proc. SPIE 3701, Orlando, FL (July 1999).

[17] Ntokas, K. F. F., Ungermann, J., Kaufmann, M., Neubert, T., and Riese, M., "Observation of horizontal temperature variations by a spatial heterodyne interferometer using single-sided interferograms," preprint, Others (Wind, Precipitation, Temperature, etc.)/Remote Sensing/Data Processing and Information Retrieval (Apr. 2023).

[18] Harris, F., "On the use of windows for harmonic analysis with the discrete Fourier transform," *Proceedings of the IEEE* **66**(1), 51–83 (1978).

[19] Naylor, D. A. and Tahic, M. K., "Apodizing functions for Fourier transform spectroscopy," *Journal of the Optical Society of America A* **24**, 3644 (Nov. 2007).

[20] Norton, R. H. and Beer, R., "New apodizing functions for Fourier spectrometry," *Journal of the Optical Society of America* **66**, 259 (Mar. 1976).

[21] Norton, R. H. and Beer, R., "Errata: New Apodizing Functions For Fourier Spectrometry," *Journal of the Optical Society of America* **67**, 419 (Mar. 1977).

[22] Boone, C. D., McLeod, S. D., and Bernath, P. F., "Apodization effects in the retrieval of volume mixing ratio profiles," *Applied Optics* **41**, 1029 (Feb. 2002).

[23] Griffiths, P. R. and De Haseth, J. A., [*Fourier transform infrared spectrometry*], Wiley-Interscience, Hoboken, N.J., 2nd ed. (2007). OCLC: 132718458.